



# Physicochemical analysis of selenium nanoparticles synthesis via pomegranate peel extracts approach: Cytotoxic impact on MCF7 cell line

Zahraa Mohammed Ahmed <sup>a,\*</sup>, Mais Emad Ahmed <sup>a</sup>

*a Department of Biology, College of Science, University of Baghdad, Jadriya, Baghdad, Iraq*

## Abstract

Over the past decade, sustainable bimetallic nanoparticles (NPs) have attracted significant scientific attention. However, challenges related to synthesis efficiency and environmental impact remain major concerns. In this study, we present the green synthesis of bimetallic selenium nanoparticles (SeNPs) using pomegranate peel extract (PPE) as a natural, eco-friendly reducing and stabilizing agent. The synthesized nanoparticles were thoroughly characterized using Fourier-transform infrared (FTIR) spectroscopy, X-ray diffraction (XRD), ultraviolet-visible (UV–Vis) spectroscopy, transmission electron microscopy (TEM), and energy-dispersive X-ray (EDX) analysis, confirming their successful formation, uniform morphology, and homogeneous distribution. The biosynthesized SeNPs demonstrated potent *in vitro* anticancer activity against the human breast cancer cell line (MCF-7), exhibiting a half-maximal inhibitory concentration (IC<sub>50</sub>) of 11 µg/mL, while remaining non-toxic and biocompatible at lower concentrations. These findings highlight the significant biomedical potential of PPE-mediated bimetallic SeNPs as safe and effective anticancer agents. Overall, this green biosynthetic approach provides a sustainable and efficient alternative to conventional chemical synthesis methods for producing functional metal oxide nanoparticles.

**Keywords:** Microbial characterization; microalgae; NCBI GenBank; growth kinetic model; biocathode; photosynthesis microbial fuel cell.

Received on 29/12/2024, Received in Revised Form on 09/04/2025, Accepted on 10/04/2025, Published on 30/12/2025

<https://doi.org/10.31699/IJCPE.2025.4.15>

## 1- Introduction

Nanoparticles are frequently used as an alternative to antibiotics to target microorganisms. Nanomaterials and nanostructures demonstrate broad-spectrum antibacterial properties [1]. Bimetallic nanoparticles (NPs), such as selenium nanoparticles (SeNPs), are known for their low cytotoxicity and promising anticancer potential. Another noteworthy example is Cu/Zn bimetallic nanoparticles synthesized using plant-based methods, which have shown a synergistic cytotoxic effect against MCF-7 breast cancer cells when combined with the anticancer drug doxorubicin, thereby enhancing therapeutic efficacy through a biocompatible and sustainable approach [2]. In light of global concerns about rising populations, it is vital to implement all agricultural measures to improve fruit and vegetable production worldwide.

Furthermore, although many fruit varieties, including bananas, watermelon, papayas, mangoes, and pineapples are appreciated for their flavor and nutrient content, over 40% of their mass, including the peel, pulp, and seeds, is inedible [3]. These NPs are produced in clean, non-toxic, and environmentally conscious ways, using high-energy renewable materials to enhance the safety and reliability of NP production processes [4]. The development of plant-fabricated NPs can proceed more rapidly because the specific media and culture conditions required for

other biological entities don't need to be maintained. Green pathway NPs often have strong catalytic capabilities, which increase toxicity in bacterial cells and cancer cells, due to their large surface areas and capacity to promote reactivity by generating reactive oxygen species [5]. Many researchers now support the use of selenium nanoparticles (SeNPs) due to their high stability and low toxicity, and they are recommended for use across a range of scientific domains [6]. Selenium nanoparticles exhibit strong adsorption and microbiological properties due to their interactions with various protein structures, compared to alternative techniques (chemical and physical).

Biologically generated SeNPs are easier to use, more environmentally friendly, and economically viable [7]. Using biomaterials like microbes, algae, biopolymers, plant materials, or their derivatives in the bio- (green) production of NPs could successfully address most of the aforementioned problems by providing a straightforward, affordable, environmentally friendly, and controllable process [8]. Sustainable bimetallic nanoparticles (NPs) have gained considerable attention over the past decade. However, challenges related to synthesis efficiency and environmental impact remain key concerns in optimizing their properties. In this study, we report the green biosynthesis of bimetallic selenium nanoparticles (SeNPs)



\*Corresponding Author: Email: [zahraa.ahmed2402m@sc.uobaghdad.edu.iq](mailto:zahraa.ahmed2402m@sc.uobaghdad.edu.iq)

© 2025 The Author(s). Published by College of Engineering, University of Baghdad.

This is an Open Access article licensed under a [Creative Commons Attribution 4.0 International License](https://creativecommons.org/licenses/by/4.0/). This permits users to copy, redistribute, remix, transmit and adapt the work provided the original work and source is appropriately cited.



using pomegranate peel extract (PPE) as an eco-friendly reducing and stabilizing agent. Characterization by ultraviolet-visible (UV-Vis) spectroscopy, Fourier-transform infrared (FTIR) spectroscopy, X-ray diffraction (XRD), transmission electron microscopy (TEM), and energy-dispersive X-ray spectroscopy (EDX) confirmed the successful synthesis of the nanoparticles [9].

Another study by [10] found that the antioxidant activity of SeNPs exceeded 90% across all tested concentrations, ranging from 250 to 4000 µg/mL. Hemocompatibility studies indicated that SeNP concentrations of 500 µg/mL or lower are safe for use. In cytotoxicity assays, SeNPs exhibited an IC<sub>50</sub> value of 113.73 µg/mL. Furthermore, SeNPs demonstrated potent anticancer activity against MCF-7 and MG-63 cancer cell lines, with IC<sub>50</sub> values of 69.8 µg/mL and 47.9 µg/mL, respectively. Therefore, in the present investigation, SeNPs with distinct anticancer properties were synthesized using crude pomegranate peel extract (PPE). Physicochemical, topographical, and biological activity evaluation tests were included in the comparative study.

## 2- Experimental work

### 2.1. PPE preparation

Fruit peels from organically grown pomegranates (*Punica granatum* L.) were manually obtained after the fruits were washed with double-distilled water (DW) and allowed to air-dry for 62 hours at  $44 \pm 2$  °C. After being mechanically ground into a powder (100 g, approximately 60 mesh size), the dried peels were extracted employing 1 L of 70% diluted ethanol, stirred at  $110 \times g$  for 65 hours at room temperature (RT;  $25 \pm 2$  °C), and filtered to get rid of any remaining plant debris. To obtain a 10% concentration, the *P. granatum* peel extract (PPE) was redissolved in DW after being vacuum-dried at 41 °C. [9]. as shown in Fig. 1.

### 2.2. Biosynthesis of PPE- Selenium nanoparticles (SeNPs)

An aqueous solution of sodium selenite, "Na<sub>2</sub>SeO<sub>3</sub>" (10 mM), was formulated with DW. A Na<sub>2</sub>SeO<sub>3</sub> solution (10 mM) and 10 ml of PPE (1%, w/v) were subsequently combined and stirred at  $610 \times g$  for 55 minutes at room temperature. The brownish-orange color of the fluid indicated the biosynthesis of SeNPs via PPE. The PPE/SeNPs matrix was precipitated from the solution by centrifugation at  $11600 \times g$  for 37 minutes. To obtain plain SeNPs, portions of the PPE/SeNPs matrix were subsequently washed three times with DW and twice with ethanol, with centrifugation performed after each wash. After that, the PPE/SeNPs and regular SeNPs were freeze-dried [11].

### 2.3. Particle size and charging

NPs Zeta (ζ) potentialities and particle size (Ps) evaluation of PPE-synthesized SeNPs and their combined

forms (PPE/SeNPs) were implemented using the DLS "dynamic light scattering" approach, employing the Zeta plus.

### 2.4. Nanoparticles ultrastructure

Using a 20 kV accelerating voltage, the SEM (scanning electron microscope) was used to examine ultrastructure, including particle topography and dispersion. TEM imaging was used to investigate further the ultrastructure of PPE-synthesized SeNPs, particularly their shape, dispersion, and Ps.

### 2.5. Characterization of SeNPs

Fourier-transform infrared spectroscopy (FTIR) (FTIR, Bruker Co., Ettlingen, Germany). SeNPs of energy dispersive X-ray (EDX), atomic force microscopy (AFM), and ultraviolet-visible spectroscopy (UV-VIS). SeNPs were measured from 200 to 600 nm using a UV-Vis spectrophotometer (UV-1800, Shimadzu, Kyoto, Japan), and X-ray diffraction (XRD) was used to investigate the shape and dimensions of the SeNPs in a powdered sample. The images were taken with a scanning electron microscope (SEM) with a resolution of 500 nm (Hitachi S-3400N). Energy-dispersive X-ray analysis EDX analysis can be used to identify the qualitative and quantitative state of elements that may be involved in the formation of nanoparticles. These examinations were conducted at the University of Baghdad's College of Sciences Department of Chemistry labs, which served [12].

#### a. Ultraviolet-visible absorption spectroscopy UV-VIS

(Shimadzu/Japan) UV-visible spectroscopy is used to quantify plasmon resonance and bulk electron oscillations in the conduction band in response to electromagnetic waves to confirm nanoparticle synthesis. It contains detailed information on the structure, size, aggregation and stability of nanoparticles. Selenium nanoparticles can be produced on a spectrophotometer in the range of 200 nm to 800 nm.

#### b. Atomic force microscopy AFM

(UNICCO/USA) was used to determine the size and surface morphology of SeNP nanoparticles. A thin layer of prepared SeNPs was deposited on a quartz glass plate by applying a few drops of SeNPs to the plate and allowing them to dry at room temperature in the dark. The lowered glass plate was then scanned with AFM.

#### c. Fourier transform infrared (FTIR) spectroscopy

Using FTIR spectroscopy, the presence of functional groups involved in the bio-reduction of SeNPs was confirmed. FTIR analysis of the chemical bonds of the



prepared SeNPs was performed by scanning in the wavelength range of 400–4000 cm<sup>-1</sup>.

#### d. Energy-dispersive X-ray analysis EDX

(Bruker/Germany) EDX analysis can be used to identify the qualitative and quantitative states of elements

that may be involved in nanoparticle formation. The element's content in selected areas within the SEM sections was examined using EDX microanalyzers. These studies have confirmed that high-purity selenium nanoparticles are generated, which depends on the interaction between the sample and the X-ray excitation sources.

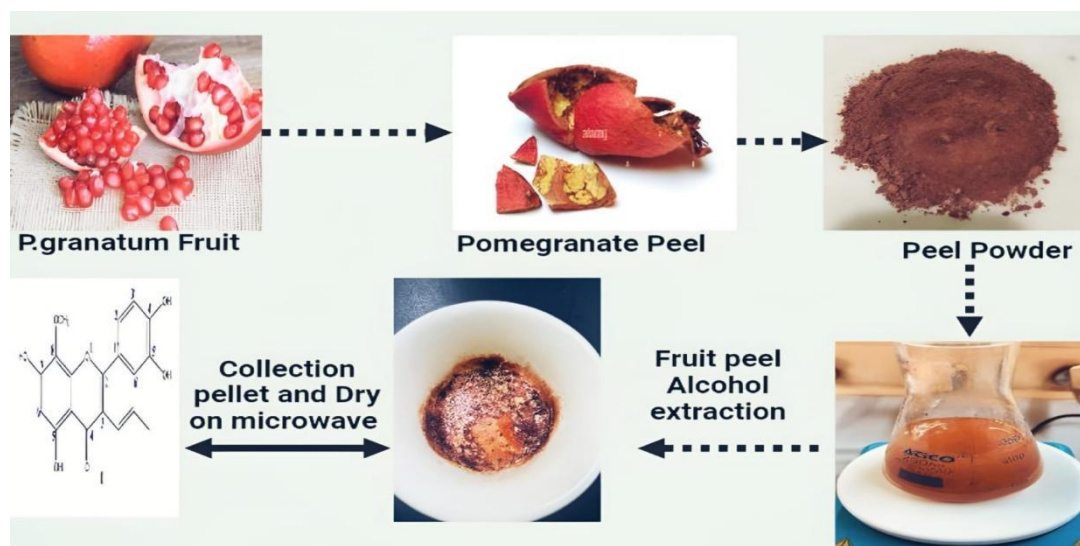


Fig. 1. PPE preparation

#### e. Field emission scanning electron microscope FESEM

(Hitachi Ltd./Japan) The images were taken with a scanning electron microscope (SEM) at 500 nm resolution (Hitachi S-3400N) and with secondary electron (BSE) detectors; quad-type semiconductor detectors were used to study the size and shape of SeNPs. This approach is used to obtain detailed information about surface NPs. This approach was used to characterize the average particle morphology and diameter of the nanoparticles. After sonication with distilled water, a tiny drop of the sample was placed on a microscope slide and left to dry. The samples were then coated with a thin layer of platinum to make them conductive.

#### f. X-ray diffraction XRD

XRD (Shimadzu/Japan) measured the crystal structure of SeNPs to investigate the shape and dimensions of the SeNPs powdered sample.

#### 2.6. Cytotoxicity assay

The cytotoxic effects were assessed using an in vitro 3-(4,5-dimethylthiazol-2-yl)-2,5-diphenyltetrazolium bromide (MTT) assay. Each well of a 96-well plate contained 7,000 MCF7 cells, which were incubated overnight to ensure cell adhesion. After that, cell lines (MCF7) were treated with substances at progressively higher SeNPs concentrations (6.25–100 µg/ml); three replicate wells were employed for each treatment. After

24 hours of incubation, the culture medium was removed from each well, and 20 µL of MTT solution (5 mg/mL; Shanghai Macklin Biochemical Co., Ltd.) was added. The plate was then incubated for 3 hours at 37 °C in the dark. Subsequently, 50 µL of DMSO (Bio Basic Inc.) was added to each well, and the plate was gently shaken for 10 minutes to dissolve the formazan crystals. [13]. Absorbance at 490 nm was measured using a microplate reader from the raw absorbance data, and the proportion of live cells was calculated using Eq. 1.

$$\text{Viability} = \frac{A_{\text{test}} - A_{\text{blank}}}{A_{\text{control}} - A_{\text{blank}}} \times 100\% \quad (1)$$

The absorbance was denoted as "A". GraphPad Prism software (version 6, Dotmatics) was used to generate the dose-response curve, from which the half-maximal inhibitory concentration (IC<sub>50</sub>), the concentration required to reduce cell viability by 50% was calculated [14].

### 3- Results and discussion

#### 3.1. Synthesis of SeNPs

The suspension's color shifts to red once Se<sub>2</sub>O<sub>3</sub> has been reduced to Se<sup>0</sup>. Observing the solution gradually change from pale yellow to a deep brownish-orange tint after 60 minutes was the first hint of the SeNPs synthesis. Several metal NPs have been biosynthesized using PPE. Significant amounts of phenolic compounds, including hydrolysable tannins and flavonoids, which are essential for the creation of metal nanoparticles, are present in pomegranate peel. PPE was used in the current



investigation to manufacture SeNPs. The biogenesis of SeNPs was indicated by the weak red, white, and red hues observed, with PPE serving as a capping or reducing agent. Bioactive phytochemicals in plant extracts act as capping agents, preventing nanoparticle agglomeration and altering their biological activity. The outcome complies with [15]. The phenolic chemicals existing in the peel of fruit, such as pomegranate (*Punica granatum* L.), comprising apigenin, caffeic acid, chlorogenic acid, cyanidin, ellagic acid, gallic acid, granatin A, granatin B, pelargonidin, punicalagin, punicalin, and quercetin, have been receiving a lot of attention in recent years. PPE-MAuNPs and PPE-MAgNPs are examples of extracts

from pomegranate peel (PPE) that support the synthesis of PPE-mediated nanoparticles (PPE-MNPs).

### 3.2. Characterization of biosynthesized SeNPS

#### a. UV-Visible (UV-VIS) spectroscopy

UV-Vis spectroscopy was used to examine the morphological characteristics of biosynthesized SeNPs, including size and shape. As shown in Fig. 2 a, an absorption peak at 217 nm for Se in sodium selenite indicates successful PPE production. In Fig. 2 b, the peak reached 362 nm. Fig. 2 c illustrates the UV-visible 283nm method used to characterize the biosynthesized SeNPs, which included individual NPs [16].

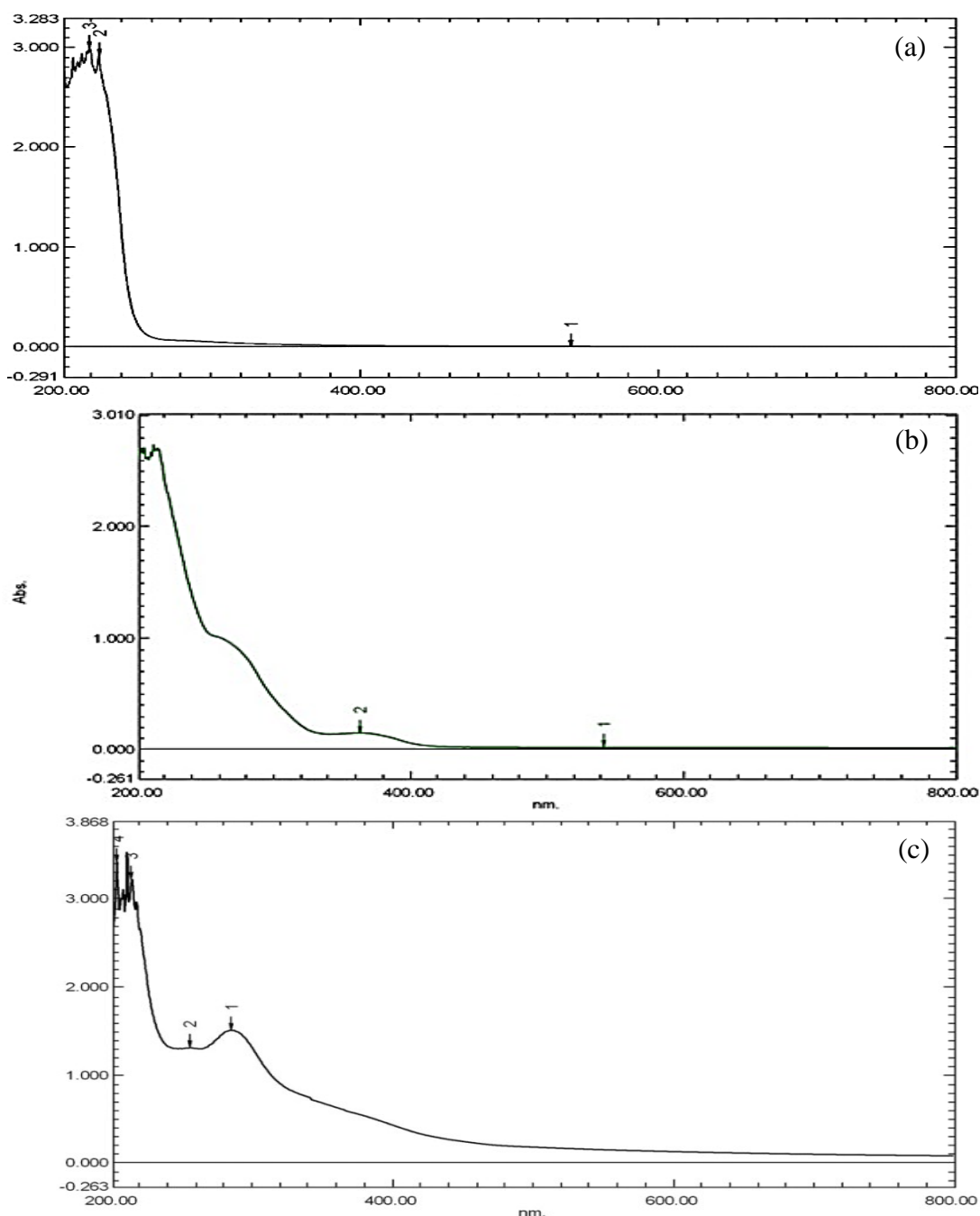


**Fig. 2.** UV—VIS spectroscopy analysis (a) pomegranate peel extract (b)  $\text{Na}_2\text{SeO}_3$  (c) Selenium nanoparticles



### b. Atomic force microscopy (AFM)

The average diameter of SeNPS, along with their two- and three-dimensional shapes, was measured using atomic

force microscopy as a confirmatory method for understanding their biogenesis in general. The study's results, displayed in Fig. 3, showed that the synthesized SeNPs had a diameter of 68 nm.

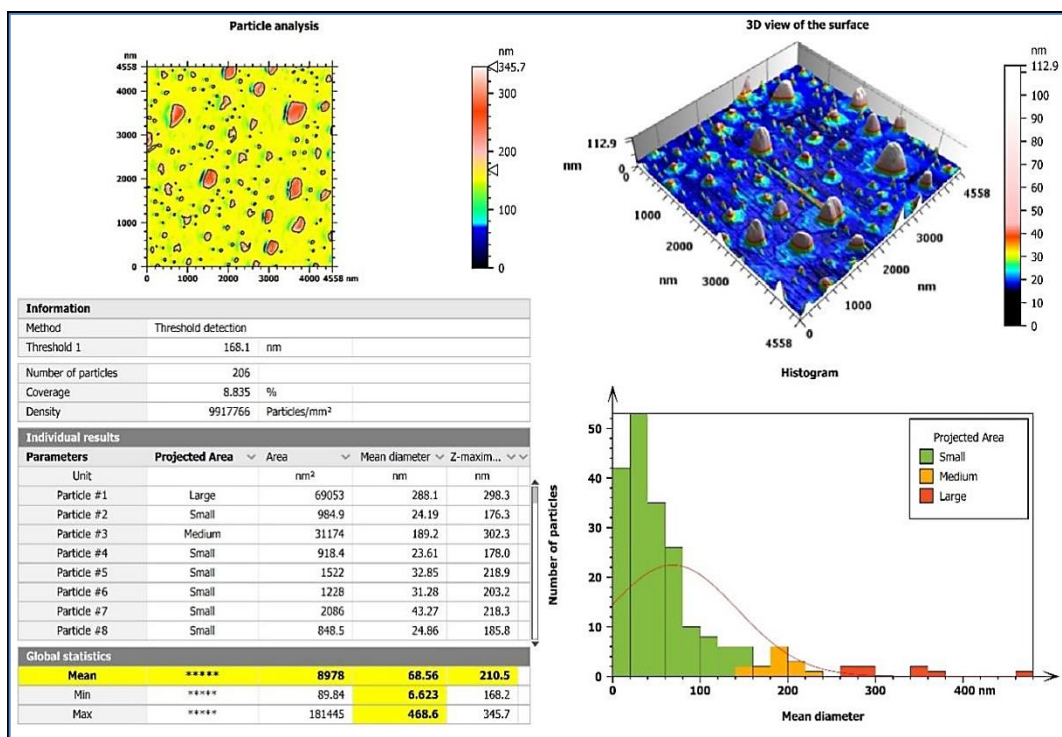


Fig. 3. The biosynthesized SeNPs under AFM, 2D and 3D images of SeNPs

### c. FTIR analysis

The PPE spectrum identified key biological linkages of the extract. The PPE spectrum's designative peaks were found at 3347, 2977, 2888, 1723, 1601, 1361, 1439, 1182, 1042, and 879 cm<sup>-1</sup> as shown in Fig. 4 a. The functional groups in PPE responsible for the biosynthesis of SeNPs were identified through the comparative spectral analysis of PPE and PPE/SeNPs, as illustrated in Fig. 4 b. The C–H stretching band observed at 2888 cm<sup>-1</sup> in the PPE spectrum nearly disappeared in the PPE/SeNPs spectrum, consistent with the findings of [17], indicating its involvement in the reduction and conjugation processes during SeNP formation. Additionally, the broad absorption band at 3426 cm<sup>-1</sup> in the PPE spectrum shifted to 3482 cm<sup>-1</sup> in the PPE/SeNPs spectrum, confirming the interaction of selenium with N–H and O–H functional groups, which play a crucial role in nanoparticle stabilization and capping.

### d. Energy dispersive X-ray (EDX)

The EDX analysis was used to determine the elemental composition of the SeNP powder. The existence of several different elements connected to the selenium, oxygen, sodium, and chloride components was determined by the EDX spectra of the SeNPs shown in Table 1 and Fig. 5. SeNPs may have coatings of carbon and oxygen. The "selenium" in the mapping pertains to

the synthesis of SeNPs, whereas the "carbon" and "oxygen" correspond to the PW extract. These findings are in line with earlier research and concur with [18].

### e. Field emission Scanning Electron Microscope (FESEM) and TEM

The SeNPs were spherical and varied in size from 10 to 60 nm, based on the TEM image shown in Fig. 6 a. TEM micrographs also demonstrated the homogeneous dispersion of the SeNPs. The SEM was used to evaluate the surface morphologies and particle sizes of SeNPs, as shown in Fig. 6 b. The shapes of SeNPs were nearly spherical. At room temperature, the Se-Nano generated from the plant extract is colloidal, with a size range of 50 to 150 nm [19]. Additionally, within the 80–220 nm range, spherical SeNPs were produced with maximum frequencies of 120–140 nm, compared with the SeNP sizes reported in the previous results, which varied from 100 to 500 nm; the SeNP size generated in this investigation is preferred [20].

### f. X-ray diffraction method (XRD)

It is abundantly evident that the initial precursors lack any distinctive peaks. Bragg's reflections at (100), (101), (111), (201), and (210) are represented by the SeNPs XRD diffraction peaks and the diffraction characteristics concerning 2θ at 23.46°, 30.08°, 41.76°, 53.12°, and



64.76°, respectively as shown in Fig. 7. We explain the results by pointing out, that previous studies have demonstrated that crystallite, cubic phase form SeNPs may be successfully fabricated at the same XRD

diffraction planes using mediators derived from plant extracts [21]. The generated SeNPs were highly crystalline to improve application, according to the XRD data.

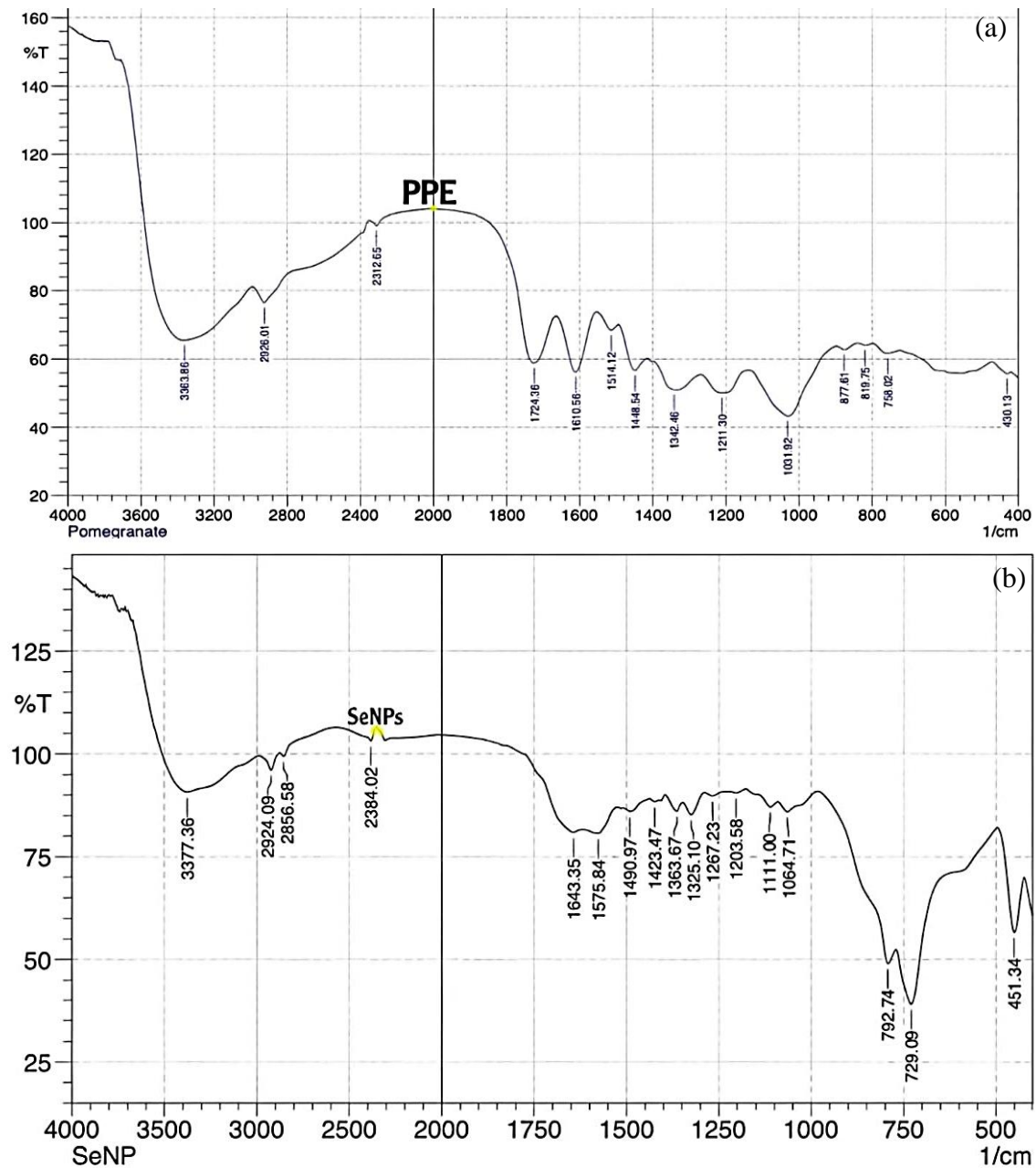
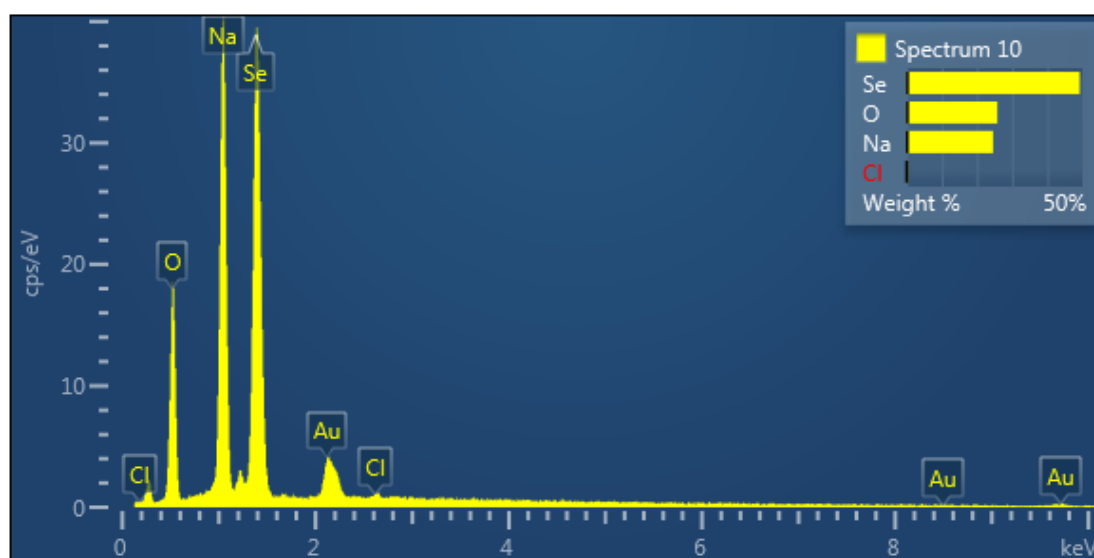


Fig. 4. FTIR spectra of (a) pomegranate peel extract (PPE) (b) SeNPs (PPE/SeNPs)

Table 1. Energy dispersive X-ray (EDX) of SeNPs

Element	Line Type	Apparent Concentration	k Ratio	Wt%	Wt% Sigma	Atomic %	Standard Label	Factory Standard
O	K series	5.01	0.01687	25.78	0.33	48.61	SiO <sub>2</sub>	Yes
Na	K series	7.01	0.02958	24.55	0.24	32.20	Albite	Yes
Cl	K series	0.08	0.00067	0.47	0.09	0.40	NaCl	Yes
Se	L series	5.87	0.05867	49.20	0.34	18.79	Se	Yes
Total:				100.00		100.00		





**Fig. 5.** The images of EDX analysis show selenium nanoparticles present with other elements

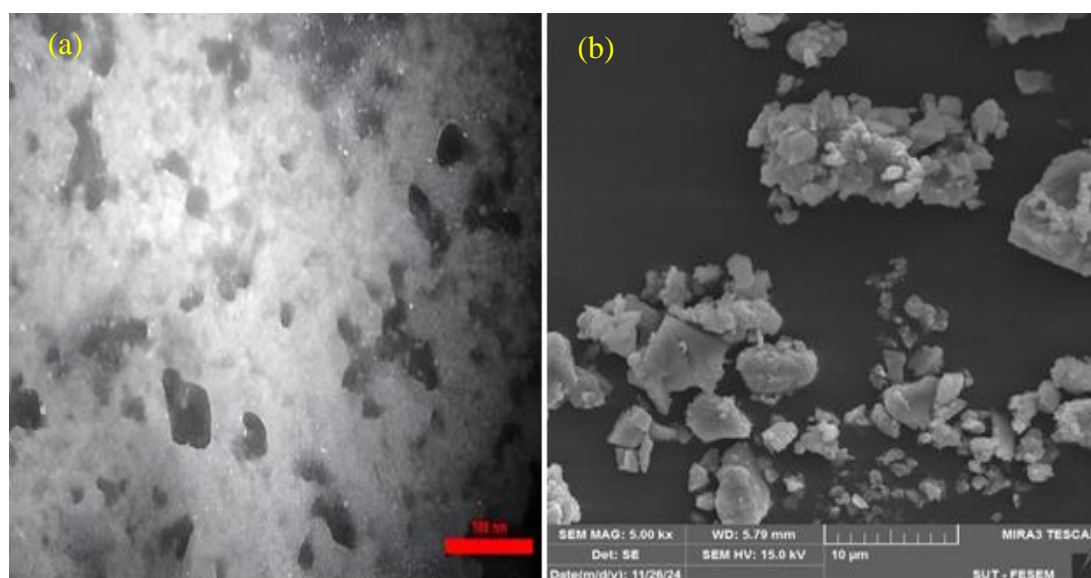


**Fig. 6.** (a) TEM image bar 100 nm (b) SEM image, of SeNPs on 5kx bar 10 µm

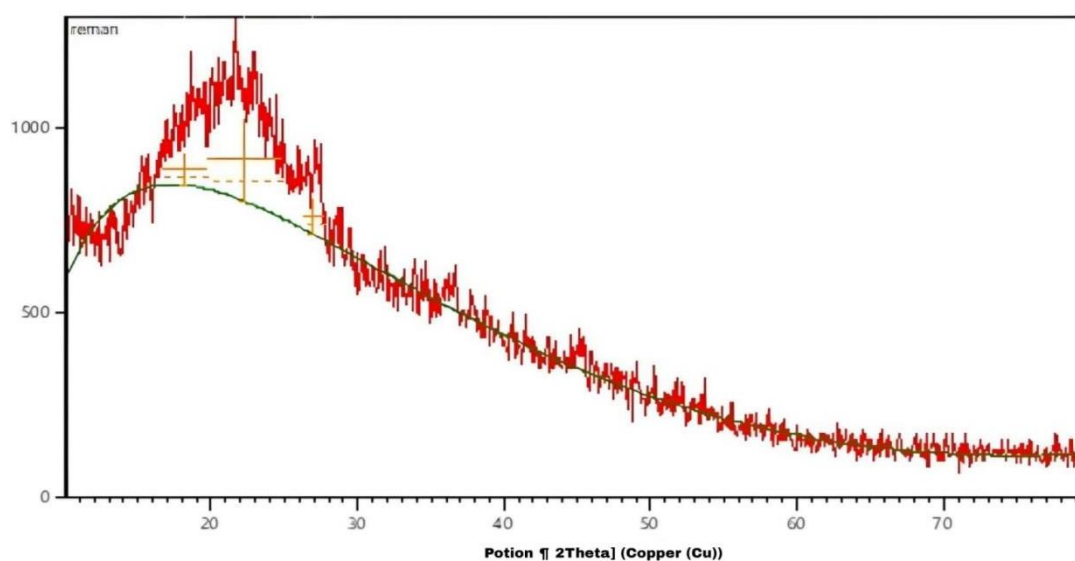


**Fig. 7.** utilizing the XRD method to analyze the structural properties (SeNPs)



## g. Zeta potential (ZP)

Depicts the diameter of PPE-SeNPs, which ranged from 75.5 to 4085.6 nm, with a mean size of 624.4 nm. Fig. 8 shows the zeta potential, which was  $-20.1$  mV. On the

other hand, 30 observed that the SeNPs made using pomegranate peel extract had a much greater zeta potential of  $-68.93$  Mv and a smaller average particle size distribution between 57.7 and 42.4 nm.

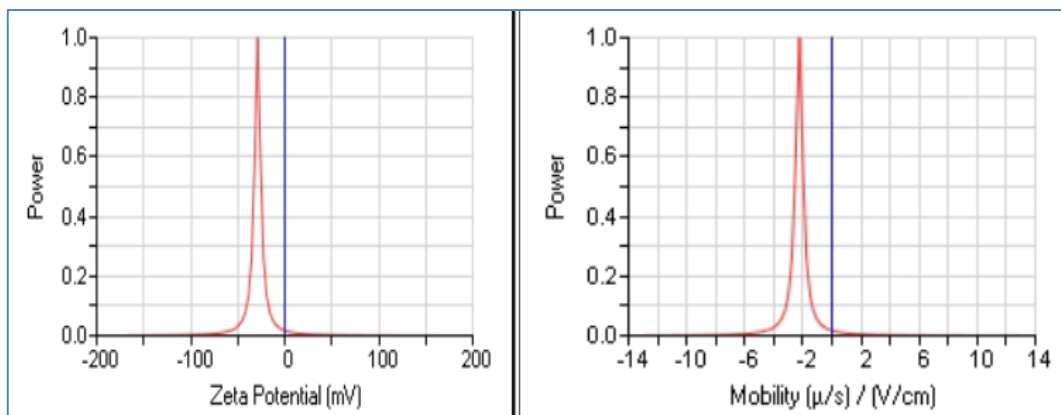


**Fig. 8.** Zeta potential of the synthesized SeNPs

### 3.3. Anticancer and Cytotoxic Activities of Biogenic Selenium Nanoparticles

The flow of materials, such as nutrients and oxygen, to tumorous tissues is enabled by the extensive vascular network and its pores [22]. It makes it simple for nanoparticles to gather and travel through these pores to

these locations. The cytotoxic activity of selenium nanoparticles on the human breast adenocarcinoma cell line MCF7 was studied, as seen in Fig. 9. It is possible to observe changes in the shape of a cell after treating it with selenium nanoparticles to compare the morphology of control cells with treated cells with two concentrations (50ug/ml and 100ug/ml).

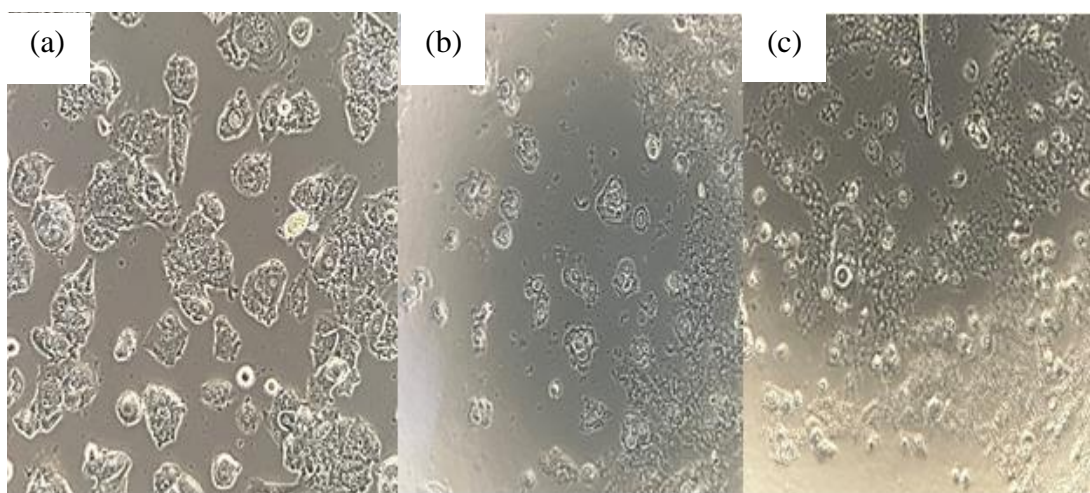


**Fig. 9.** The cytotoxic effect of SeNPs at 200× magnification (a) Control MCF7 cell (b) MCF7 cells after treatment with SeNPs at a concentration of 50  $\mu\text{g/ml}$  (c) MCF7 cells after treatment with SeNPs at a concentration of 100  $\mu\text{g/ml}$

Studies have indicated that as the concentration of SeNPs, cell viability declined, SeNPs had a  $\text{GI}_{50}$  value of nearly  $11 \mu\text{g/ml}$ . These nanoparticles exhibited significant cytotoxicity against the MCF-7 cell line, with cytotoxicity reaching 65.4% at 25  $\mu\text{g/mL}$ . SeNPs were evaluated for in vitro cytotoxicity against MCF-7 cells across a concentration range of 6.25–100  $\mu\text{g/mL}$ . Consistent with our findings, several studies have also reported the cytotoxic potential of SeNPs against various cancer cell lines.

Table 2 demonstrates the interactions amongst the cell lines illustrated in Fig. 10, at various amounts of SeNPs

(6.25–100  $\mu\text{g/ml}$ ), expressed as cell viability (%). In every instance, as nanoparticle concentration increases, the cell viability ratio decreases. The result agrees with [23]. The cytotoxicity of chemically synthesized SeNPs was significantly lower than that of the corresponding chemical controls. This study aimed to investigate the cytotoxic and apoptotic effects of selenium nanoparticles on cancer cell lines, specifically MCF-7 (breast cancer) and HepG2 (liver cancer) cells. Transmission electron microscopy (TEM) analysis confirmed that the SeNPs were approximately 20 nm in size, with predominantly spherical and cubic morphologies, and exhibited well-



defined crystalline characteristics. The cytotoxic potential of SeNPs was assessed using MTT and NRU assays, revealing that both cell lines displayed variable sensitivity to SeNP-induced cytotoxicity, highlighting differences in their response to selenium nanoparticle treatment [24]. The primary cytotoxicity mechanism of SeNPs is the

generation of intracellular ROS, leading to cell death and mitochondrial dysfunction. The mitochondria control the apoptosis process, however SeNPs can cause apoptosis by changing the Bcl-2 protein, which weakens the outer membrane of the mitochondria and progressively speeds up the death process [25].

**Table 2.** The cytotoxicity of SeNPs on cell line MCF7 raw data, the viability %

		CV	6.25 ug/ml	12.5 ug/ml	25 ug/ml	50 ug/ml	100ug/ml
SeNPs	Raw data	0.305	0.245	0.113	0.275	0.263	0.257
TR1	% survival	100	80.32786885	37.04918033	90.16393443	86.2295082	84.26229508
SeNPs	Raw data	0.305	0.275	0.13	0.305	0.277	0.268
TR2	% survival	100	90.1639344	42.6229508	100	90.81967	87.86885
SeNPs	Raw data	0.305	0.275	0.129	0.283	0.278	0.257
TR3	% survival	100	90.1639344	42.295082	92.78689	91.14754	84.2623

CV: Control vehicle, TR: Technical replicate

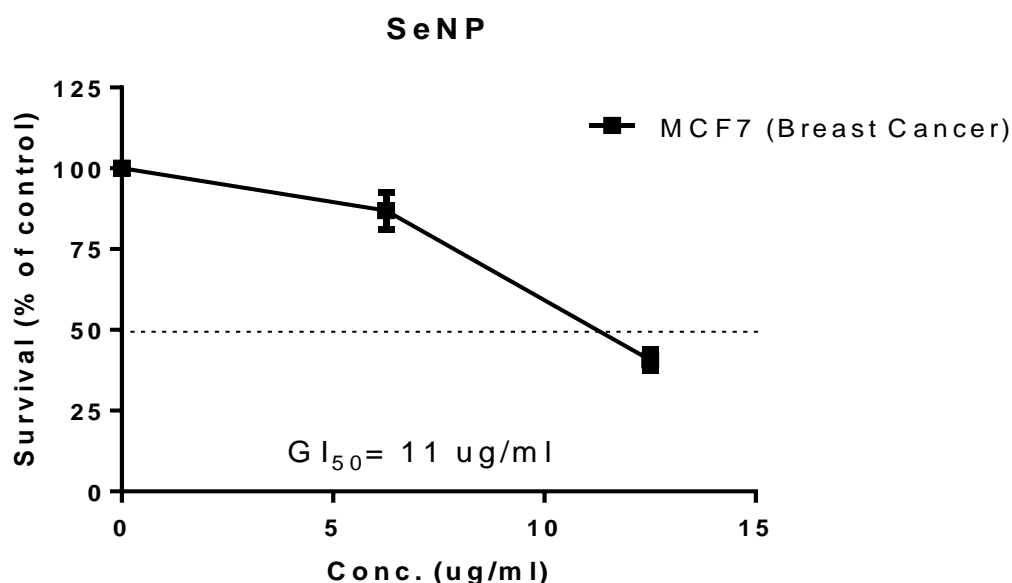


**Fig. 10.** The cytotoxic effect of SeNPs on MCF7 cells

#### 4- Conclusion

Selenium nanoparticles (SeNPs) exhibit significant antioxidant and anticancer properties and have also been explored as dietary supplements. Numerous toxicity studies have demonstrated that SeNPs are relatively safe when administered at appropriate doses. Future research should focus on advancing characterization techniques, exploring their potential in targeted drug delivery systems, and improving green synthesis methods to enhance scalability and sustainability. SeNPs are significant nanoparticles with a wide range of medical uses. Interest in these techniques is heightened by the bioactive properties of SeNPs produced via green synthesis and their biocompatible architectures. SeNPs were created in this work using a simple, inexpensive, and environmentally friendly process. The synthesis-derived Pv-SeNPs' characteristics were assessed using XRD, EDX, UV-vis, TEM, AFM, DLS, and TGA-DTA data. Nanoparticle characteristics, including concentration, size, shape, surface charge, interaction time, and degree of deposition, all affect toxicity. Chemical adsorption, electrostatic attraction, hydrophobic interaction, or

chemical bonding are how nanoparticles interact with cells.

#### References

- [1] A. H. Hashem, M. A. AlAbboud, M. M. Alawlaqi, T. M. Abdelghany, and M. Hasanin. Synthesis of Nanocapsules Based on Biosynthesized Nickel Nanoparticles and Potato Starch: Antimicrobial, Antioxidant, and Anticancer Activity. *Starch-Stärke*, 74, 2100165, 2021. <https://doi.org/10.1002/star.202100165>
- [2] F. A. Zadeh, D. O. Bokoy, O. D. Salahdin, W. K. Abdelbasset, M. A. Jawad, M. M. Kadhim, and M. Khatami. Cytotoxicity evaluation of environmentally friendly synthesis Copper/Zinc bimetallic nanoparticles on MCF-7 cancer cells. *Rendiconti Lincei. Scienze Fisiche e Naturali*, 33(2), 441-447, 2022. <https://doi.org/10.1007/s12210-022-01064-x>



- [3] M. E. Ahmed, G. M. Sulaiman, B. A. Hasoon, R. A. Khan, and H. A. Mohammed. Green Synthesis and Characterization of Apple Peel-Derived Selenium Nanoparticles for Anti-Fungal Activity and Effects of MexA Gene Expression on Efflux Pumps in *Acinetobacter baumannii*. *Applied Organometallic Chemistry*, e7805. 2024. <https://doi.org/10.1002/aoc.7805>
- [4] A.M.H. Al-Rajhi, S.S. Salem, A.A. Alharbi, and T.M. Abdelghany. Ecofriendly synthesis of silver nanoparticles using Kei-apple (*Dovyalis caffra*) fruit and their efficacy against cancer cells and clinical pathogenic microorganisms. *Arabian Journal of Chemistry*, 15, 103927. 2022. <https://doi.org/10.1016/j.arabjc.2022.103927>
- [5] M.A. Elkodous, H.M. El-Husseiny, G.S. El-Sayyad, A.H. El-Sayyad, A.S. Doghish, D. Elfadil, Y. Radwan, H.M. El-Zeiny, H. Bedair, and O.A. Ikhdair. Recent advances in waste-recycled nanomaterials for biomedical applications: Waste-to-wealth. *Nanotechnology Reviews*, 10, 1662–1739. 2021. <https://doi.org/10.1515/ntrev-2021-0099>
- [6] A. H. Hashem, T. A. Selim, M. H. Alruhaili, S. Selim, D. H. M. Alkhalifah, S. K. Al Jaouni, and S. S. Salem. Unveiling antimicrobial and insecticidal activities of biosynthesized selenium nanoparticles using prickly pear peel waste. *Journal of Functional Biomaterials*, 13(3), 112, 2021. <https://doi.org/10.3390/jfb13030112>
- [7] S.S. Salem, M.S.E.M. Badawy, A.A. Al-Askar, A.A. Arishi, F.M. Elkady, and A.H. Hashem. Green Biosynthesis of Selenium Nanoparticles Using Orange Peel Waste: Characterization, Antibacterial and Antibiofilm Activities against Multidrug-Resistant Bacteria. *Life*, 12, 893, 2022. <https://doi.org/10.3390/life12060893>
- [8] M. Emad, and K.Salama. A comparison of the effects of lemon peel-silver nanoparticles versus brand toothpastes and mouthwashes on staphylococcus spp. isolated from teeth caries. *Iraqi Journal of Science*, 61(8), 1894-1901, 2020. <https://doi.org/10.24996/ij.s.2020.61.8.6>
- [9] M. F. Salem, W. A. Abd-Elraoof, A. A. Tayel, F. M. Alzuair, and O. M. Abonama. Antifungal application of biosynthesized selenium nanoparticles with pomegranate peels and nanochitosan as edible coatings for citrus green mold protection. *Journal of Nanobiotechnology*, 20(1), 182, 2022. <https://doi.org/10.1186/s12951-022-01393-x>
- [10] A. H. Hashem, E. Saied, O. M. Ali, S. Selim, S. K. Al Jaouni, F. M. Elkady, and G. S. El-Sayyad. Pomegranate peel extract stabilized selenium nanoparticles synthesis: promising antimicrobial potential, antioxidant activity, biocompatibility, and hemocompatibility. *Applied Biochemistry and Biotechnology*, 195(10), 5753-5776, 2023. <https://doi.org/10.1007/s12010-023-04326-y>
- [11] S. Menon, H. Agarwal, S. Rajeshkumar, P.J.Rosy, and V.K. Shanmugam. Investigating the antimicrobial activities of the biosynthesized selenium nanoparticles and its statistical analysis. *Bionanoscience*, 10:122 –35. 2020. <https://doi.org/10.1007/s12668-019-00710-3>
- [12] M. F. Salman, N.H.A.L. Al-Mudallal, and M.E. Ahmed. The effect of selenium nanoparticles on the expression of MexB gene of *Pseudomonas aeruginosa* Isolated from wound and burn infections. *Iraqi JMS*; 22 (1): 79-92. 2024.
- [13] Z. J. S. Hassan, M. K. Hamid, and M. E. Ahmed. Synthesized Zinc Oxide Nanoparticles by the Precipitation Method on Streptococcus spp. from Dental Carries and Cytotoxicity Assay. *International Journal of Drug Delivery Technology* 12, 1327-1330. 2022. <https://doi.org/10.25258/ijddt.12.3.65>
- [14] S.M. Mahdi, A.F. Abbas, and M.E. Ahmed. Cytotoxicity of zinc oxide nanoparticles to lymphocytes using Enterococcus faecium bacteriocin and assessment of their antibacterial effects. *Nanomedicine Research Journal*. Apr 1;9 (2):180-94. 2024. <https://doi.org/10.22034/nmrj.2024.02.007>
- [15] P. Monika, M. N. Chandrababha, R. Hari Krishna, M. Vittal, C. Likhitha, N. Pooja, and V. Chaudhary. Recent advances in pomegranate peel extract mediated nanoparticles for clinical and biomedical applications. *Biotechnology and Genetic Engineering Reviews*, 40(4), 3379-3407, 2024. <https://doi.org/10.1080/02648725.2022.2122299>
- [16] A. H. Hashem, A. A. Al-Askar, M. R. Al-Askar, K. A. Abd-El salam, A. S. El-Hawary, and M. S. Hasanin. Sustainable biosynthesized bimetallic ZnO@ SeO nanoparticles from pomegranate peel extracts: antibacterial, antifungal and anticancer activities. *RSC advances*, 13(33), 22918-22927. 2023. <https://doi.org/10.1039/D3RA03260D>
- [17] S. Potrč, T. Kraševac Glaser, A. Vesel, N. Poklar Ulrih, Z. L. Fras. Two-layer functional coatings of chitosan particles with embedded catechin and pomegranate extracts for potential active packaging. *Polymers*, 12 (9):1855. 2020. <https://doi.org/10.3390/polym12091855>
- [18] A.H. Hashem, S.S. Salem. Green and ecofriendly biosynthesis of selenium nanoparticles using *Urtica dioica* (stinging nettle) leaf extract: Antimicrobial and anticancer activity. *Biotechnology Journal*, 17, 2100432.2022. <https://doi.org/10.1002/biot.202100432>
- [19] R. Avendaño, N. Chaves, P. Fuentes, E. Sánchez, J.I. Jiménez, M. Chavarria. Production of selenium nanoparticles in *Pseudomonas putida* KT2440. *Scientific Reports*, 6, 37155. 2016. <https://doi.org/10.1038/srep37155>



- [20] F. H. Fawzi, and, M. E. Ahmed. Green Synthesis and Characterization of Selenium Nanoparticles via Staphylococcus warneri Approach: Antimicrobial and on PhzM Pyocyanin Gene Expression in Pseudomonas aeruginosa. *Plasmonics*, 1-17. 2025. <https://doi.org/10.1007/s11468-024-02378-2>
- [21] B. Wang, K. Zhang, J. Wang, R. Zhao, Q. Zhang, and X. Kong. Poly (amidoamine)-modified mesoporous silica nanoparticles as a mucoadhesive drug delivery system for potential bladder cancer therapy. *Colloids and Surfaces B: Biointerfaces*, 189:110832. 2020. <https://doi.org/10.1016/j.colsurfb.2020.110832>
- [22] R. A. Fernandes, A. A. Fernandes, E. C. Torres, A. F. M. Buszinski, G. L. Fernandes, C. C Mendes-Gouvêa, and D. B. Mendes-Gouvêa. Antimicrobial potential and cytotoxicity of silver nanoparticles phytosynthesized by pomegranate peel extract. *Antibiotics*, 7(3), 51, 2018. <https://doi.org/10.3390/antibiotics7030051>
- [23] X.F. Zhang, Z.G. Zhang, W. Shen, and S. Gurunathan. Silver Nanoparticles: Synthesis, Characterization, Properties, Applications, and Therapeutic Approaches. *International journal of molecular sciences*, 17. 2016. <https://doi.org/10.3390/ijms17091534>
- [24] K.X. Lee, K. Shameli, Y.P. Yew, S.Y. Teow, H. Jahangirian, R. Rafee-Moghaddam, and Webster T.J. Webster. Recent developments in the facile biosynthesis of gold nanoparticles (AuNPs) and their biomedical applications. *International Journal of Nanomedicine*, 275–300. 2020. <https://doi.org/10.2147/IJN.S233789>
- [25] M. F. Baran, C. Keskin, A. Baran, K. Kurt, P. İpek, A. Eftekhari, and W. C. Cho. Green synthesis and characterization of selenium nanoparticles (Se NPs) from the skin (testa) of Pistacia vera L.(Siirt pistachio) and investigation of antimicrobial and anticancer potentials. *Biomass Conversion and Biorefinery*, 1-11, 2024. <https://doi.org/10.1007/s13399-023-04366-8>



## التحليل الفيزيائي الكيميائي لتخليق جسيمات السيلينيوم النانوية من خلال مستخلصات قشر الرمان و التأثير السام على خط خلايا MCF7

زهراء محمد احمد<sup>١</sup>،\*، ميس عماد احمد<sup>١</sup>

<sup>١</sup> قسم علوم الحياة، كلية العلوم، جامعة بغداد، بغداد، العراق

### الخلاصة

في السنوات العشر الماضية، حظيت الجسيمات النانوية ثنائية المعدن المستدامة (NPs) باهتمام كبير. ومع ذلك، يرتبط تركيبها وتحسين خصائصها بقضايا الكفاءة والبيئة. هنا، نصف التركيب الحيوي الأخضر والصدى للبيئة لجسيمات SeNP ثنائية المعدن باستخدام مستخلص قشر الرمان (PPE). الهدف من دراسة مستخلص نباتي من قشور الرمان (PPE) وجسيمات نانوية من السيلينيوم مُصنَّعة حيويًا باستخدام PPE (PPE/SeNPs) واقترحت كتأثير فعال في تقليل التأثير السام للخلايا على خط خلايا MCF7. ساهمت الأشعة تحت الحمراء لتحويل فورييه (FTIR) و الحيود بالأشعة السينية (XRD) والأشعة فوق البنفسجية المرئية (UV-vis) و المجهر الإلكتروني النافذ (TEM) و طيف EDX في نجاح التركيب. يتراوح الحد الأدنى للتركيز المثبط (MIC) المقابل لجسيمات SeNP ثنائية المعدن بين ١٠٠٠ و ٦٤ ميكروغرام/مل. أظهرت الجسيمات النانوية خصائص توزيع متجانسة وجيدة. أظهرت نشاطاً قوياً مضاداً للسرطان في المختبر ضد خط خلايا سرطان الثدي البشري MCF7، الجسيمات النانوية ثنائية المعدن غير سامة وآمنة للاستخدام في الطب الحيوي عندما يكون نصف تركيزها المثبط الأقصى ( $IC_{50}$ ) أكبر من ١١ ميكروغرام / مل، وفقاً لنتائج السمية الخلوية. كانت الإمكانيات الهندسية الطبية الحيوية لـ SeNPs ثنائية المعدن التي تم تصنيعها حيويًا بشكل فعال باستخدام PPE كبيرة. يعد التخليق الحيوي لجسيمات أكسيد المعدن النانوية بديلاً ممتازاً لعملية التخليق الكيميائي. تهدف الدراسة الحالية إلى إنشاء تخليق أخضر وصديق للبيئة لمستخلص قشر الرمان (PPE).

الكلمات الدالة: السمية الخلوية، مستخلص قشر الرمان، سيلينيوم، حيود الاشعة السينية.